Supplemental Material:

Methods

Plasmid Construction and Lenti-virus preparation

The BoNT/C1 light chain (genebank number X53751.1, residues 1-449) had been subjected to codon optimization in mammalian cells by GenScript (*1*). Site-directed mutagenesis was performed on the BoNT/C1 light chain in a syn-lox lenti-viral vector (*2*). The syn-lox construct, along with two other viral envelope protein encoding vectors, VSVg and delta 8.9, were co-transfected into HEK cells using calcium phosphate. The HEK cells were cultured for another 3-4 days to grow up lentivirus. The supernatant was collected, filtered to remove cell particles, centrifuged at 20,000 rpm for two hours to concentrate the virus, and dissolved in 100 µl PBS (Cellgro, 21-040-CV; Manassas VA) per 30 ml supernatant.

Protein expression and western blot

For BoNT/C1 LC expression, 5 µl lenti-virus-PBS was added to each well of a 24-well plate of cultured hippocampal neurons at 10-12 days *in vitro*. After 72-96 hours, lysates from cultured neurons were prepared by first washing cells with PBS. Lysis buffer (100 µl 1% Triton X-100, 0.05% SDS, and protease inhibitors in PBS) was added and lysates were collected, vibrated for 10 minutes, and centrifuged for 10 min (*1*). The supernatants were collected and incubated with SDS loading dye containing 1 mM DTT at 95 ^{o}C for 5 minutes. Samples were subjected to SDS-PAGE and blotted with antibodies against SNAP-25 (Cl. 71.1, SySys, Gottingen, Germany) and syntaxin (HPC-1, SySys). Monoclonal antibody against β–actin was purchased from Abcam (ab6276-100).

Expression in PC12 cells was achieved by electroporation (ECM 830; BTX, Hawthorne NY) of the lenti-viral syn-lox DNA.

Cell culture

For primary cultured hippocampal neurons, hippocampi from E-18 embryonic rats were dissected and digested with trypsin for 30 minutes followed by trituration (*3*). The cell suspension was plated on poly-D-lysine coated cover slips in Neurobasal-A Medium (600 µl/well of a 24-well plate) together with B27 and 2 mM Glutamax, and culture in a humidified 95% air/5% CO_2 incubator. PC12 cells were cultured in DMEM, 5% horse serum, and 5% iron-supplemented calf serum in 10 cm plates at 37 ℃ in 90% air/10% CO_2 (*4*).

Electrophysiology

Whole-cell patch clamp recordings were performed with an Axon Instruments Axopatch 200B amplifier (*3*). Cultured hippocampal neurons were bathed with an external solution containing 140 mM NaCl, 5 mM KCl, 5 mM $CaCl_2$, 1 mM $MgCl_2$, 10 mM HEPES, and 10 mM glucose (pH 7.4, 300 mOsm). Sylgard-coated (Sylgard 184 kit; Dow Corning, Midland, MI) patch electrodes were filled with 130 mM K-Gluconate, 10 mM EGTA, 5 mM HEPES, 5 mM phosphocreatine, 2 mM Mg-ATP, 0.3 mM Na-GTP (pH=7.3). EPSCs were evoked by extracellular stimulation of cultured

neurons patch clamped with the same pipette solution given above but with 5 mM QX-314 (lidocaine N-ethyl bromide). For miniature EPSCs, 1 μM TTX was added to block action potentials; 50 μM D-AP5 (D-2-amino-5-phosphonopentanoate) was added to block NMDA receptors, and 100 μM picrotoxin was added to block GABA receptors. The stimulation electrode was filled with external solution. The neurons were held at a membrane potential of -70 mV. Current was digitized with a digidata interface and read into a PC with PClamp software (Molecular Devices). Data were analyzed with MiniAnalysis software (Synaptosoft), Clampfit (Molecular Devices), and Origin (Microcal). The data were presented as the mean ± SEM. The student's *t*-test was used to calculate the p values and presented as: **p<0.01, *** p<0.001.

Amperometry

PC12 cells were loaded overnight by addition of 1.5 mM norepinephrine and 0.5 mM ascorbate to the culture medium. Cells expressing the BoNT/C1 light chain construct were selected in a fluorescence microscope using the dsRed fluorescent protein present in the syn-lox vector. Norepinephrine release was recorded with a VA-10X amperometry amplifier (ALA Scientific, Farmingdale, NY) using 5-μm carbon fiber electrodes held at 650 mV (*4*). Cells were bathed in a solution containing 150 mM NaCl, 4.2 mM KCl, 1 mM NaH_2PO4, 0.7 mM $MgCl_2$, 2 mM $CaCl_2$, and 10 mM HEPES (pH 7.4). Secretion was evoked by pressure ejection (for 6 seconds) from a micropipette (1-2 μm tip, ~10 μm away from the cell) of a solution identical to the bathing solution but with 105 mM KCl and 5 mM NaCl.

Supplemental Mutagenesis Data

We have performed an extensive mutagenesis study of BoNT/C1 light chain. Three mutants were used to explore the role of syntaxin in Ca^{2+}-triggered exocytosis, and these results are presented in the main body of this work. Results from the many other mutants we generated are presented here in this supplement in order to provide insight into structure-function relations in the BoNT/C1 light chain and its interactions with substrates. The results presented indicate the qualitative catalytic efficacy of the various mutants. However, BoNT/C1 light chain expression levels were not assayed independently, so that low syntaxin and SNAP-25 cleavage could reflect poor expression of a particular mutant. Furthermore, the structural integrity of the mutants was not evaluated and misfolding of mutants cannot be ruled out.

BoNT/C1 cleaves SNAP-25 between residues R198 and A199, one peptide bond before the BoNT/A cleavage site. BoNT/C1 cleaves syntaxin 1A between residues K253 and A254 and syntaxin 1B between residues K252-A253**.** Fig. 1A highlights four distinct domains with important roles in enzymatic activity (*5, 6*). Residues H229, H233, E269 coordinate a zinc ion to form the active site (Fig. 1A, gold region). The S1' pocket, formed by L200, M221, I226, H229, and R372, holds the substrate in position. Residues R372 and Y375 play a critical role in generating the transition state. A region we refer to as the γ-exosite includes S51, R52, and N53, and is involved in substrate recognition.

The three synaptic SNAREs are cleaved by 8 different clostridial neurotoxins at sites indicated in Fig. S1A. In the BoNT/A light chain residues Arg362 and Tyr365 were found to be directly involved in catalysis by stabilizing the transition state (*5*). By alignment with the BoNT/C1 light chain, we identified the equivalent residues Arg372 and Tyr375 (Fig. S1B). We mutated one or both of these residues, and they dramatically diminished the catalytic activity of BoNT/C1 (Fig. S1C). Since these homologous residues share similar roles, we continued to use the BoNT/A-substrate complex crystal structure (Fig. S1B) to guide us in the selection of residues for mutagenesis in the BoNT/C1 light chain.

BoNT/C1 recognizes the P1' sites in homologous locations in its two major substrates. In syntaxin, the P1' site is A254, and in SNAP25 the P1' site is A199. We found that the putative S1' pocket of BoNT/C1 (Fig. S2A) plays an important role in the proteolysis of both syntaxin and SNAP25. This most likely reflects a role for the cavity in optimizing interactions between the active site and substrate P1' site. The putative S1' pocket is formed by Pro168, Leu200, Met221, Ile226, His229, Arg372 (*6*). Mutations in Pro168, His229, Arg372 destroyed proteolytic activity, while mutations on Leu200, Met221 and Ile226 showed different effects (Fig. S2B). Most interestingly, the triple mutant of 200W-221W-226W (BoNT/C1α-3W) cleaved syntaxin as well as wild type BoNT/C1 but did not cleave SNAP-25. Based on these results, we identified a series of mutations that cleave only syntaxin (Fig. S2C). These results suggest that these three residues function together in substrate recognition.

However, mutations in the putative substrate binding regions, the α and β exosites, failed to alter protease activity, which suggests that substrate recognition probably depends on other sites. In the BoNT/A light chain, the '250 loop' formed antiparallel β sheets together with SNAP-25, which is important for the interaction in the β exosites (*7*). However, mutations in the corresponding '250 loop' region in the BoNT/C1 light chain do not alter protease activity (Fig. S3). The α exosite is thought to serve as a remote substrate binding site that places the substrate in an optimal orientation for hydrolysis. The α-exosite contains residues Lys 346 and Lys 365 which could form hydrogen bonds with residues Asp 166 and Gln 152 of SNAP-25 (Fig. S4A). However mutating these residues either individually (Fig. S4B) or together (Fig. S4C) had little or no effect on enzymatic activity.

We identified two regions that reduce SNARE protein cleavage, and although poor expression or misfolding of some of the mutants has not been ruled out, these sites appear to have profound effects on BoNT/C1 activity. One such site is the 'paddle' region containing a sheet of four β strands (Fig. S5A,B). Mutating these β sheet residues completely abolished catalytic activity. So this region is important for both syntaxin and SNAP-25 cleavage. We designate residues Ser51, Arg52 and Asn53 as the 'γ exosite', and propose that it has a role in SNAP-25 recognition. The 'γ exosite' refers to. Mutating these residues to 51Thr, 52Asn and 53Pro yielded another series of syntaxin specific toxins Bont/C1α-51 (Fig. S2C).

These findings reveal a number of interesting structure-function relations in the BoNT/C1 light chain, and shed light on its mechanisms of proteolytic activity and substrate recognition. The information should be useful in developing vaccines and inhibitors of BoNT/C1.

Table Legend

Table S1. Cleavage assay results for 151 BoNT/C1 constructs. The table lists the specific mutants that were assayed, grouped according to region/domain and presents cleavage in neurons for both syntaxin and SNAP-25. The relative activity for each construct was scored +, through +++++, with o denoting no detectable activity. Western blots for selected mutants were presented in Figs. S1-S5 and discussed in the text.

Figure Legends

Figure S1. Cleavage of endogenous syntaxin and SNAP-25 by BoNT/C1 light chain in cultured rat hippocampal neurons.

A. The substrates of the botulinum neurotoxin (BoNT) family. (Modified from ref. (*8*)). **B**. The structure of BoNT/C1 light chain (*6*). A black dashed curve indicates the putative site of SNAP-25 binding. **C**. Wild type BoNT/C1 light chain cleaves syntaxin into several shorter peptides, and cleaves SNAP-25 to a peptide with a molecular mass of ~24 kD. Residues 372 and 375 are critical in producing the transition state, and mutating one or both blocks cleavage.

Figure S2. Mutations in the putative S1' pocket.

A. Structure as in Fig. 1b highlighting the S1' pocket. **B**. Mutating S1' residues decreased enzyme activity. Leu200 and Met221 mutations retain some enzymatic activity for both syntaxin and SNAP-25, while the Ile226W mutation abolished activity. However, the 200trp-221trp-226trp triple mutant (designated BoNT/C1α-3W) only cleaved syntaxin 1A and 1B. **C**. Other mutations showed similar selectivity for syntaxin (designated BoNT/C1α forms).

Figure S3. Mutations in the β-exosite (250 loop).

A. Structure as in Fig. 1b highlighting the 250 loop. The crystal structure suggested that this loop, designated the β-exosite, is essential for substrate binding. **B**. The potential scissile bond proximal substrate binding region in the 250 loop does not affect enzymatic activity. Other mutations in this region gave similar results (see Table).

Figure S4. Mutations in the α-exosite.

A. Structure as in Fig. S1b highlighting the α-exosite. Residues Lys346 and Lys365 are part of the α-exosite and could form hydrogen bonds with Asp166 and Gln152 of SNAP-25. **B**. Mutations of Lys346 and Lys365 had no effect on activity. **C**. Double mutations in these α-exosite residues also had no effect on activity.

Figure S5. Mutations in the putative 'paddle' and γ-exosite.

A. Close to the S1' pocket, SNAP-25 and syntaxin could 'wrap' around the 'paddle'

(four β-sheets). **B**. Residues 48-66 (the γ-exosite) are in the SNAP-25 binding site. Mutations in residues colored green had no effect on enzyme activity. Mutations of residues colored red cleave both SNAP-25 and syntaxin. Mutations of residues colored magenta only diminished SNAP-25 cleavage. **C**. Mutations in the 'paddle' show no enzyme activity. These mutations might disrupt the local structure and prevent the substrate from binding correctly.

References

1. Dong, M., Tepp, W. H., Liu, H., Johnson, E. A., and Chapman, E. R. (2007) Mechanism of botulinum neurotoxin B and G entry into hippocampal neurons, *J Cell Biol 179*, 1511-1522.
2. Gascon, S., Paez-Gomez, J. A., Diaz-Guerra, M., Scheiffele, P., and Scholl, F. G. (2008) Dual-promoter lentiviral vectors for constitutive and regulated gene expression in neurons, *J Neurosci Methods 168*, 104-112.
3. Wang, D., Zhang, Z., Chanda, B., and Jackson, M. B. (2010) Improved probes for hybrid voltage sensor imaging, *Biophys J 99*, 2355-2365.
4. Zhang, Z., Hui, E., Chapman, E. R., and Jackson, M. B. (2009) Phosphatidylserine regulation of Ca^{2+}-triggered exocytosis and fusion pores in PC12 cells, *Mol Biol Cell 20*, 5086-5095.
5. Binz, T., Bade, S., Rummel, A., Kollewe, A., and Alves, J. (2002) Arg(362) and Tyr(365) of the botulinum neurotoxin type a light chain are involved in transition state stabilization, *Biochemistry 41*, 1717-1723.
6. Jin, R., Sikorra, S., Stegmann, C. M., Pich, A., Binz, T., and Brunger, A. T. (2007) Structural and biochemical studies of botulinum neurotoxin serotype C1 light chain protease: implications for dual substrate specificity, *Biochemistry 46*, 10685-10693.
7. Breidenbach, M. A., and Brunger, A. T. (2004) Substrate recognition strategy for botulinum neurotoxin serotype A, *Nature 432*, 925-929.
8. Sutton, R. B., Fassauer, D., Jahn, R., and Brunger, A. T. (1998) Crystal structure of a SNARE complex involved in synaptic exocytosis at 2.4 Å resolution, *Nature 395*, 347-353.

Table 1

Domain	Mutation	syntaxin activity	SNAP-25 activity
transition state	372A	o	o
	372A-375F	o	o
S1 pocket	200W	+++	+++
	200E	+++	+++
	200R	+++	+++
	221W	+++	+++
	221E	+++	+++
	221R	+++	+++
	226A	+++++	+++++
	226C	+++++	++++
	226D	++++	++
	226E	+++++	+++++
	226F	+++	+
	226G	+++++	+++++
	226H	+++	++
	226K	+++	+
	226L	++++	++++
	226M	++++	++
	226N	+++++	++++
	226P	+++	+
	226Q	++++	++
	226R	+++	+
	226S	+++++	++++
	226T	+++++	+++++
	226V	++++	++++
	226W	o	o
	226Y	++++	++
	200W-221W	+++	+++
	221R-226R	o	o
	200E-221E	+++	+++
	168E-200E-221E	o	o
	168R-221R-226R	o	o
	168W-221W-221W	o	o
	200R-221R-226R	o	o
	200E-221E-226E	o	o
	200W-221W-226W	+++	o

	200W-221W-226A	+++	++
	200W-221W-226C	+++	++
	200W-221W-226D	++	+
	200W-221W-226E	++	+
	200W-221W-226F	+++	+++
	200W-221W-226G	+++	+++
	200W-221W-226H	+++	o
	200W-221W-226K	+++	o
	200W-221W-226L	+++	o
	200W-221W-226M	+++	+++
	200W-221W-226N	+++	+++
	200W-221W-226P	+++	++
	200W-221W-226Q	+++	+++
	200W-221W-226R	+++	++
	200W-221W-226S	+++	+++
	200W-221W-226T	+++	+++
	200W-221W-226V	+++	+++
	200W-221W-226Y	++	+
	168W-200W-221W-226W	o	o
	168R-200R-221R-226R	o	o
	168E-200E-221E-226E	o	o
	200W-220W-221W-222W-226W	o	o
	200W-216A-217G-218K-221W-226W	++	o
	200W-216W-217W-218W-221W-226W	o	o
	200W-216A-217A-218A-221W-226W	++	o
α– exosite	346A	+++++	+++++
	346E	+++++	+++++
	346R	+++++	+++++
	346Q	+++++	+++++
	346W	+++++	+++++
	365A	+++++	+++++
	365E	+++++	+++++
	365W	+++++	+++++
	365R	+++++	+++++
	365Q	+++++	+++++
	346A-365E	+++++	+++++
	346A-365Q	+++++	+++++
	346A-365W	+++++	+++++
	346A-365R	+++++	+++++
	346E-365A	+++++	+++++
	346Q-365A	+++++	+++++
	346W-365A	+++++	+++++

	346R-365A	+++++	+++++
	346E-365E	+++++	+++++
	346A-365A	++++	++++
	346R-365R	+++++	+++++
	316S-317delete-318delete	+++++	+++++
250 loop-β exosite	244N-245P-246N	+++++	+++++
	249delete-250F-251K	+++++	+++++
	262G-263L-264E	+++++	+++++
	266E-267Y-268K	+++++	+++++
	266E-267Y-268K-270I-271Y-272A	+++++	+++++
	24I-25P-26delete	+++++	+++++
γ–exosite	66Q-67V-68P	+++++	+++++
	63E-64A-65K	+++++	+++++
	59D-60D-61D	+++++	+++++
	54E-55E-56G-57D	+++++	+++++
	54R-55R-56R	+++++	+++++
	54T-55Q-55N	+++++	+++++
	54W-55W-56W	+++++	+++++
	54A-55A-56A	+++++	+++++
	51R-52R-53R	+++++	+
	51D-52D-53D	+++++	+
	51T-52N-53P	+++++	o
	50R-51T-52N	+	o
	50Y-51T-52N	+++	o
	50D-51T-52N	+	o
	51T	+++++	++++
	51V	+++++	++++
	51W	+++++	++++
	50D	++	++
	50E	++	++
	50W	++++	++++
	48E	+++++	+++++
	48N-49Q-50L	o	o
	49-insertDT-50	+	+
	48-insertDT-49	o	o
	49-insertDT-50-54E-55E-56G-57D	o	+
	48-insertDT-49-54E-55E-56G-57D	o	o
	49K-50Y-54E-55E-56G-57D	o	o
	49D-50D-54E-55E-56G-57D	o	o
	49D-50D-54E-55E-56G-57D	+	+

	49-insertR-50-54E-55E-56G-57D	+	+
	49-insertD-50-54E-55E-56G-57D	+	+
	49-insertT-50-54E-55E-56G-57D	+	+
	49-insertFS-50-54E-55E-56G-57D	+++++	+++++
	51T-52N-53P-200W-221W-226W	+	o
	49-insertDT-50-51T-52N-53P-54E-55E-56G-57D	o	o
β-paddle	42R-43R-44R	o	o
	158R-159R	o	o
	170R-171R-172R	o	o
	192W-193W-194W	o	o
	167R-168R-169R	o	o
	43R-44R	o	o
	43W-44W	o	o
	193W-194F	+	+
	193R-194F	+	+
	167Q-168F	+++	++
	170C-171K-172F	+++	++
	167Q-168F-170C-171K-172F	++	+
	193D	++++	+++
	167W-168W-169W	o	o
putative contact	119G-120delete-121delete	+++++	+++++
regions	203E-204E-205S	+++++	+++++
	135C-135I-135N	+++++	+++++
	145delete-146delete-147Y	+++	++
	119G-120delete-121delete-145delete-146delete-147Y	+	+
	145delete-146delete-147Y-150E-151E-152delete-153delete	o	o
	200T-201F-202G	+	+
	216A-217G-218K	+++	++
	224A-225V-226T	o	o
	224A-225V-226T-235G-236H-237R	o	o
Bont/A chimeras	BA1-165+BC169-430	o	o
	BA1-222+BC229-430	o	o
	BA1-268+BC276-430	o	o

Figure S1

A

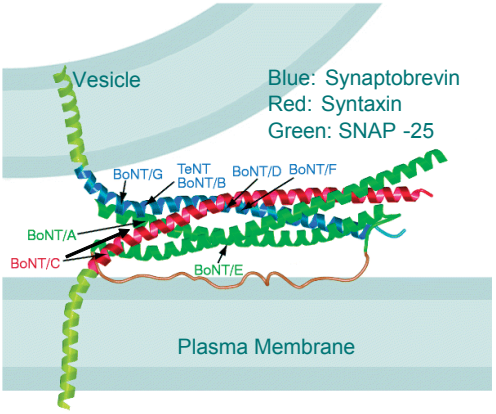

B

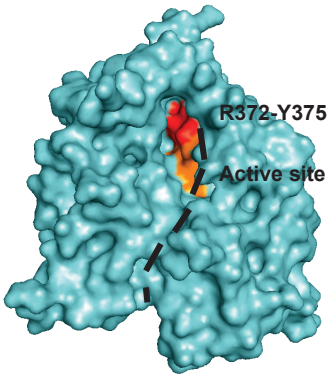

C

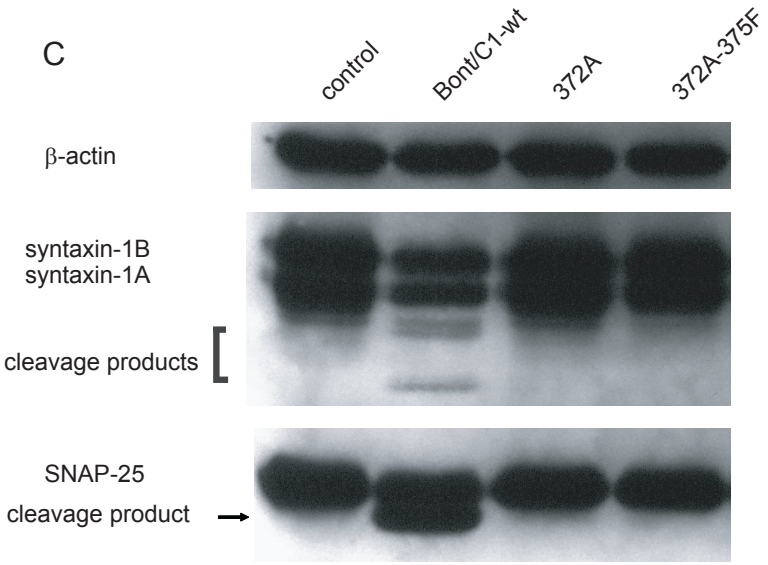

Figure S2

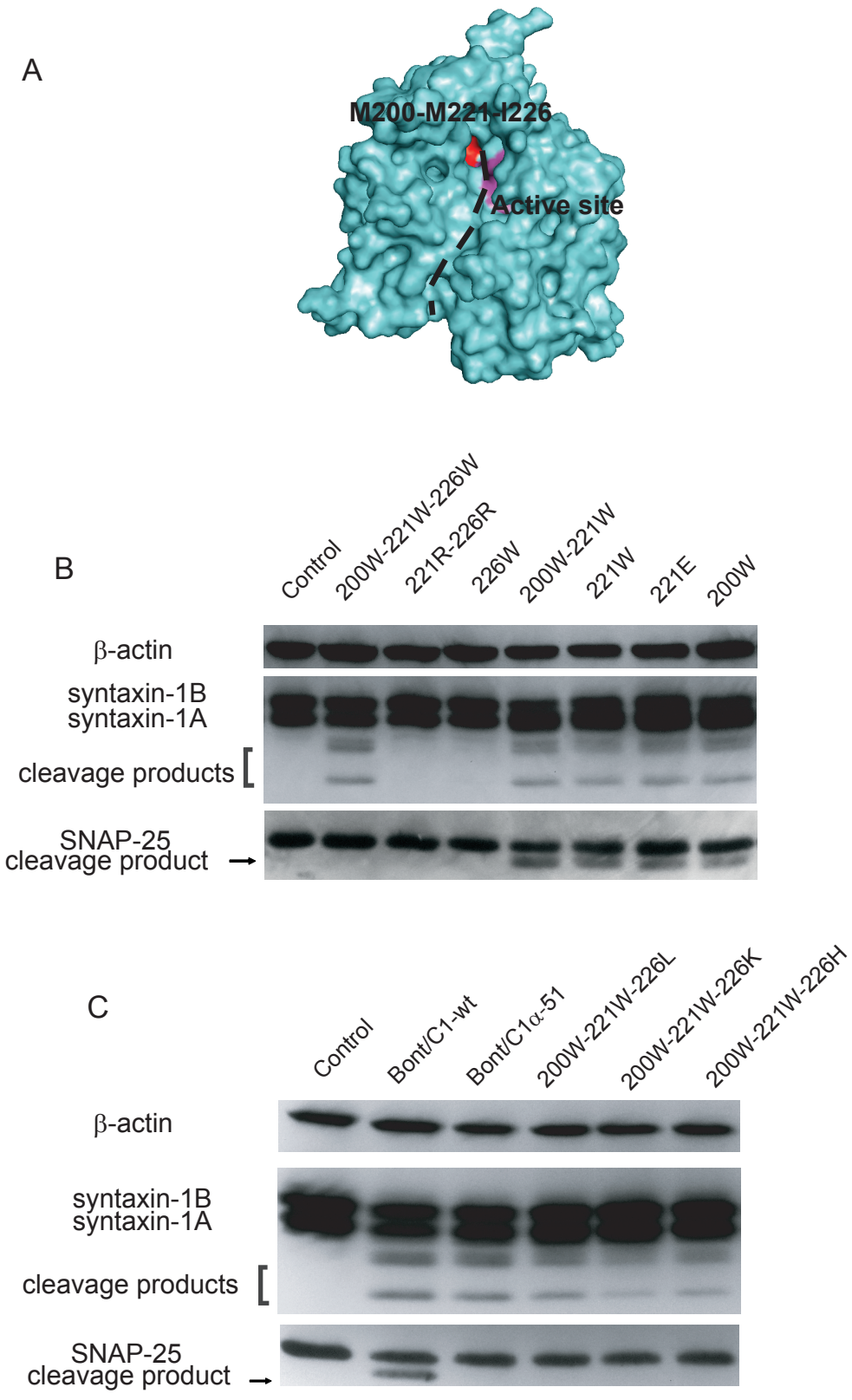
A
M200-M221-I226
Active site
B
Control
200W-221W-226W
221R-226R
226W
200W-221W
221W
221E
200W
β-actin
syntaxin-1B
syntaxin-1A
cleavage products
SNAP-25
cleavage product
C
Control
Bont/C1-wt
Bont/C1α-51
200W-221W-226L
200W-221W-226K
200W-221W-226H
β-actin
syntaxin-1B
syntaxin-1A
cleavage products
SNAP-25
cleavage product

Figure S3

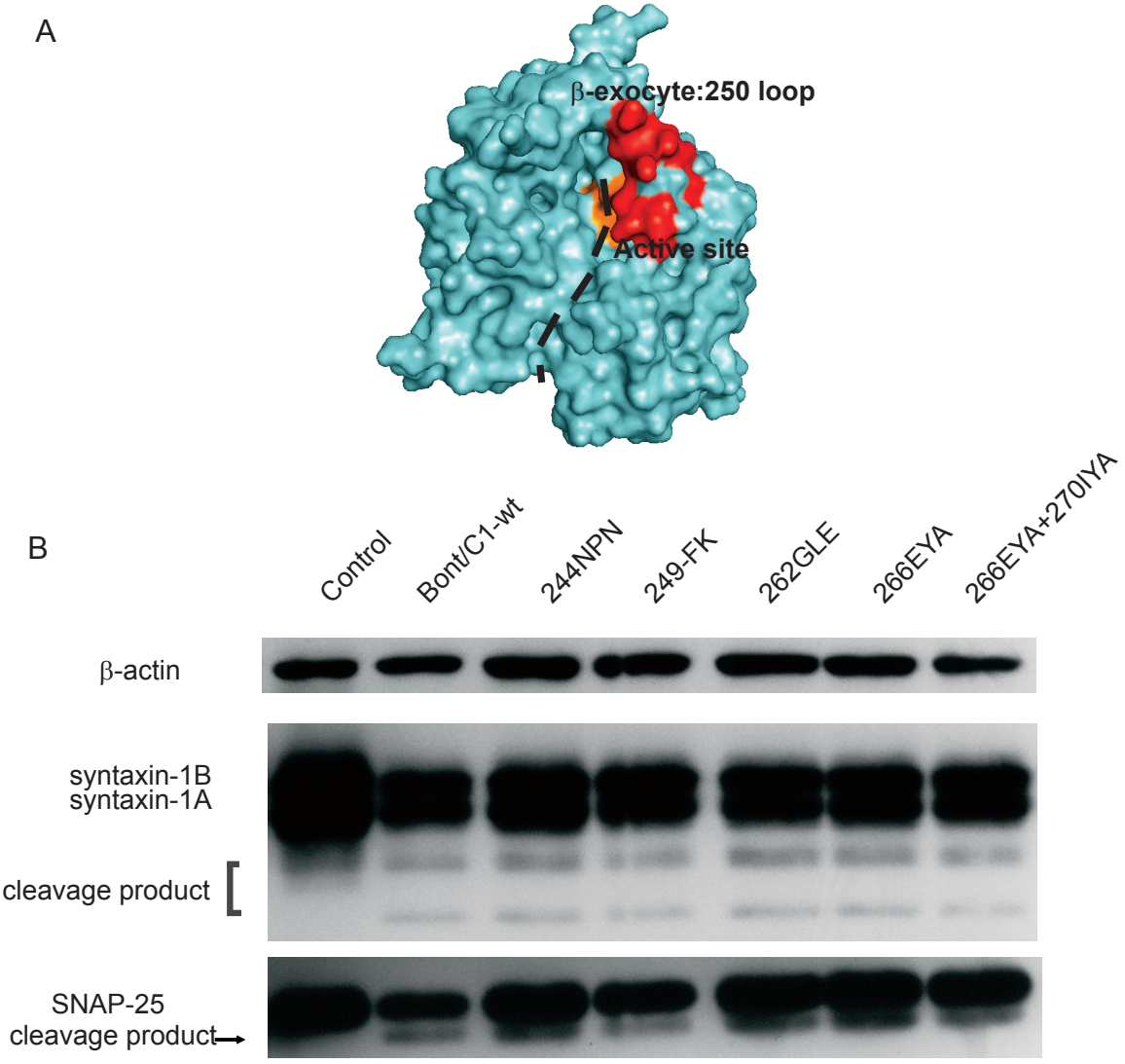
A
β-exocyte:250 loop
Active site
B
Control
Bont/C1-wt
244NPN
249-FK
262GLE
266EYA
266EYA+270IYA
β-actin
syntaxin-1B
syntaxin-1A
cleavage product
SNAP-25
cleavage product

Figure S4

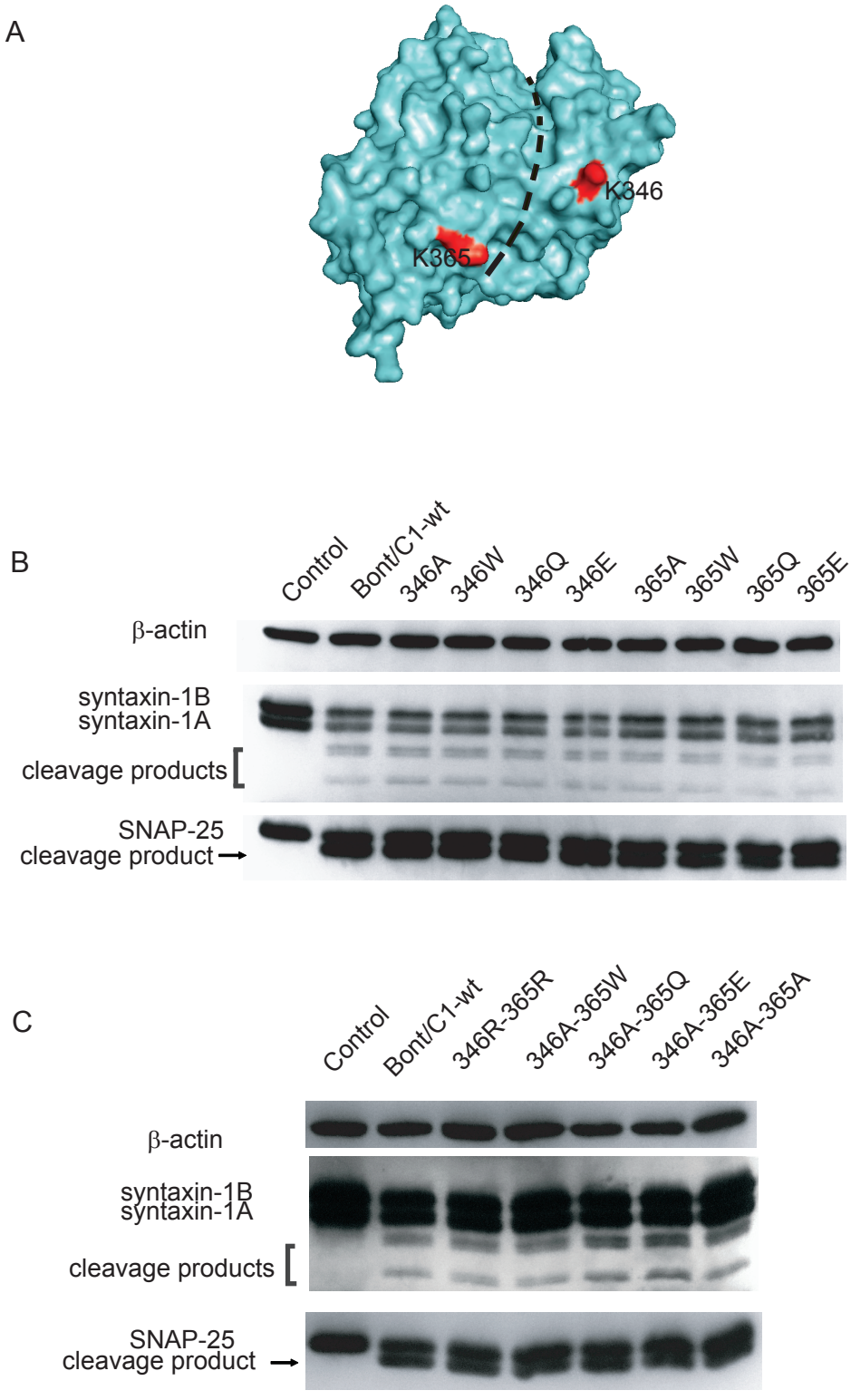
A
K346
K365
B
Control
Bont/C1-wt
346A
346W
346Q
346E
365A
365W
365Q
365E
β-actin
syntaxin-1B
syntaxin-1A
cleavage products
SNAP-25
cleavage product
C
Control
Bont/C1-wt
346R-365R
346A-365W
346A-365Q
346A-365E
346A-365A
β-actin
syntaxin-1B
syntaxin-1A
cleavage products
SNAP-25
cleavage product

Figure S5

A

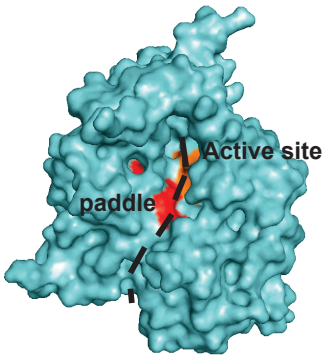

B

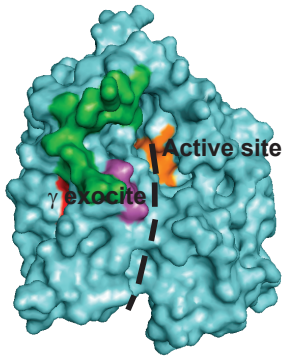

C